buildings

MDPI

Article

Experimental Application of Cement-Stabilized Pavement Base with Low-Grade Metamorphic Rock Aggregates

Qian Yang [1], Yi Liu [2,*], Haotian Zou [2], Xiaoxiong Wang [2], Guohuan Gong [2], Yinnan Cheng [2], Liang Zhang [3] and Zhengwu Jiang [1]

[1] Key Laboratory of Advanced Civil Engineering Materials of Ministry of Education, School of Materials Science and Engineering, Tongji University, Shanghai 201804, China; yqtumutj@163.com (Q.Y.); jzhw@tongji.edu.cn (Z.J.)
[2] Guizhou Hongxin Chuangda Engineering Detection & Consultation Co., Ltd., Guiyang 550014, China; an_kong22@163.com (H.Z.); sxdthywxx@126.com (X.W.); guohuan_gong@163.com (G.G.); yn_cheng97@163.com (Y.C.)
[3] Guizhou Transportation Planning Survey & Design Academe Co., Ltd., Guiyang 550081, China; zhang123liang2022@163.com
* Correspondence: yliuzm@163.com

Abstract: Low-grade metamorphic rock (LMR) is a kind of stone that is widely distributed in China. The alkali activity strictly prevents its application in conventional concrete. This paper evaluates the possibility of using LMR aggregate in cement-stabilized pavement base (CSPB). The compressive strength of CSPB prepared with LMR and limestone aggregates at various curing conditions was measured. Expansion rates were determined via accelerated simulation tests to assess the alkali reactivity of LMR, followed by microscopic analysis. Finally, the possibility of using LMR in CSPB was evaluated from the economic viewpoint. Results indicate that CSPB specimens prepared with LMR have similar compressive strength at each content of cement, regardless of curing conditions. The expansion rates of all CSPB specimens with LMR were lower than 0.1%, indicating the absence of an AAR, which was further validated by the absence of the AAR product in microscopic observations. It is inferred from the economic analysis that 70.9% lower cost can be achieved by the replacement of limestone aggregate with LMR aggregate. This demonstrates that technical, economic and environmental benefits endow LMR with wide market potential as the aggregate of CSPB.

Keywords: alkali–aggregate reaction; low-grade metamorphic rock; cement-stabilized pavement base; strength; microstructure

check for updates

Citation: Yang, Q.; Liu, Y.; Zou, H.; Wang, X.; Gong, G.; Cheng, Y.; Zhang, L.; Jiang, Z. Experimental Application of Cement-Stabilized Pavement Base with Low-Grade Metamorphic Rock Aggregates. *Buildings* **2022**, *12*, 589. https://doi.org/10.3390/buildings12050589

Academic Editor: Jian-Guo Dai

Received: 10 March 2022
Accepted: 27 April 2022
Published: 2 May 2022

Publisher's Note: MDPI stays neutral with regard to jurisdictional claims in published maps and institutional affiliations.

Copyright: © 2022 by the authors. Licensee MDPI, Basel, Switzerland. This article is an open access article distributed under the terms and conditions of the Creative Commons Attribution (CC BY) license (https://creativecommons.org/licenses/by/4.0/).

1. Introduction

Alkali–aggregate reaction (AAR) is an expansive reaction between alkali-active mineral components and the soluble alkaline solution from cement and admixtures in concrete pores [1–4]. Since AAR products have a strong water swelling capability, the expansion stress generated in the swelling process may exceed concrete strength, which, therefore, can further cause cracking damage to the concrete structures [5]. AAR is a global problem, and there are varying degrees of damage caused by AAR in all countries in the world. In 1940, the United States first discovered an AAR damage to a road in Bradley, California [6]. In the 1850s, Denmark surveyed 431 concrete buildings across the country, of which, 34% had suffered varying degrees of AAR damage, and 15% were completely destroyed. Since then, the United Kingdom, France, Australia, Spain, Switzerland, and Canada have all discovered cases of AAR causing concrete structure damage [7]. In 1990, there were many reports of AAR damage in China. AAR accidents occurred in Beijing, Tianjin, Shandong, Shaanxi, Inner Mongolia, Henan and other places. The damaged projects involved overpasses, airports, concrete bridges, railway sleepers, and civil buildings. Relevant investigations and studies have shown that the alkali content of cement is generally high in China, especially in the northern regions, and alkali-reactive aggregates are widely distributed [8–13].

Low-grade metamorphic rock (LMR) is a resource of manufactured sand, widely distributed in China with a large reserve. Using these LMRs as aggregates for concretes can reduce costs and alleviate the crisis of river sand resource shortages. However, the potential for alkali reactivity has been found in LMR aggregates [1,14–17]. If LMR is directly used without taking any action, the reactivity will cause concrete to expand and crack, posing a serious threat to the safe operation of the infrastructure. Consequently, it is very important and crucial to prevent and detect the alkali–aggregate reactivity of LMR aggregates [18,19]. Currently, there are severe application problems for the use of LMRs and a need to quickly evaluate their alkali reactivity and effectively prevent and control these harmful reactions when they are used as concrete aggregates.

Three well-known basic conditions are necessary to trigger the alkali–aggregate reaction in concrete, including a humid environment, and the presence of active aggregates and free alkali [20]. This means AAR can be avoided if the free alkali content is controlled. From this viewpoint, LRM has the potential to be used in cement-stabilized pavement base (CSPB), given that the free alkali is mainly from cement, and the amount of cement in CSPB is quite low.

Therefore, this paper evaluates the possibility of LMR aggregates for the preparation of CSPB. The strength, expansion behavior and micromorphology of cement-stabilized pavement base with low-grade metamorphic rock (LMR-CSPB) are tested. The economic benefit of using LMR in CSPB is also analyzed.

2. Materials and Methods

2.1. Materials

The 42.5 grade Ordinary Portland cement (P.O 42.5 Retarded cement) from Southwest Cement Co., Ltd. (Kaili, China), was used in this investigation. The properties of the cement are listed in Table 1, and its chemical composition is shown in Table 2.

Table 1. Physical properties of cement.

Normal Consistency (%)	Alkali Content (%)	Specific Surface Area (m^2/kg)	Setting Time (min)		Compressive/Flexural Strength (MPa)	
			Initial	Final	3d	28d
27.1	0.56	330	206	421	19.1/4.3	46.6/10.8

Table 2. The chemical composition of cement (wt%).

SiO_2	Al_2O_3	Fe_2O_3	CaO	MgO	SO_3	Loss
23.10	6.21	4.05	59.60	3.18	1.82	2.03

LMR aggregates were provided by Shi Jiangchong quarry (Kaili, China) in the southeast area of Guizhou Province, China. Crushed low-grade metamorphic rock with four particle size grades, i.e., 20–30 mm, 10–20 mm, 5–10 mm and 0–5 mm are used, the particle size distribution is listed in Table 3. The alkali activity of the LMR in the Shi Jiang Chong quarry was judged by the rapid mortar rod method, and a total of 137 groups of LMR rocks were sampled and tested for the alkali activity during different time periods between May 2017 and July 2019, which can indicate the fluctuation of the alkali activity of the LMR rock. The monitoring results of the alkali activity of the LMR in the Shi Jiang Chong quarry are illustrated in Figure 1. It can be seen that the 14 days-expansion rate of LMR is basically between 0.1% and 0.2%, and the expansion rate of almost all specimens is less than 0.3%, which meets the requirement in TB/T 3275 [21].

Table 3. The size distribution of LMR aggregates.

Type of Aggregate	Particle Size /mm	Sieve Size (mm)/Accumulated Screening Rate (%)												
		31.5	**26.5**	**19**	**16**	**13.2**	**9.5**	**4.75**	**2.36**	**1.18**	**0.6**	**0.3**	**0.15**	**0.075**
LMR	20~30	2.5	60.8	97.4	99.5	100								
	10~20		1.6	9.4	56.6	79.2	98.5	99.9	100					
	5~10				0.8	5.3	51.6	99.1	99.8	100				
	0~5							1.6	33.5	47.1	70.5	81.8	87.6	92.5

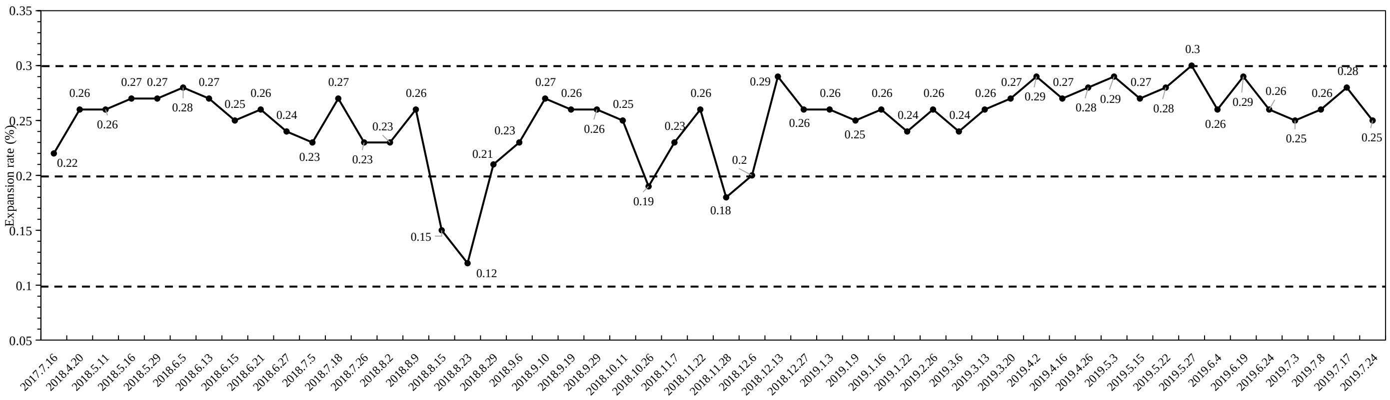

Figure 1. The monitoring results of the alkali activity of LMR.

Crushed limestone rock is used for comparison in this investigation. The gradation of limestone coarse aggregate and fine aggregate was adjusted to be the same as that of LMR rock aggregates to avoid the influence of different gradations on the test results when designing the experiment. The physical properties of LMR aggregates and limestone aggregates are shown in Tables 4 and 5. The basic performance indexes of coarse aggregate and fine aggregate of shallow metamorphic rock meet the requirements in the JTG/T F20 [22], and these can therefore be used as aggregate to prepare CSPB material.

Table 4. The physical properties of LMR coarse aggregate.

Type of Aggregate	Particle Size /mm	Apparent Density (kg/m^3)	Crushing Value (%)	Elongated or Flat Particle (%)	Water Absorption (%)	Soft Stone Content (%)	Less than 0.075 mm Particles (%)
LMR	20~30	2.712	15.3	16.4	0.2	1.8	0.6
	10~20	2.741		17.4	0.3	2.3	0.9
	5~10	2.687		19.8	0.6	2.8	1.2
Limestone	20~30	2.763	12.2	11.5	0.2	1.2	0.4
	10~20	2.801		11.8	0.2	1.6	0.7
	5~10	2.722		18.8	0.4	1.8	0.9
Requirements in JTG/T F20-2015		/	≤26	≤20	/	≤3	≤2

Table 5. The physical properties of LMR fine aggregate.

Type	Requirements in JTG/T F20-2015	LMR	Limestone
MB value (g/kg)	/	0.75	0.75
Powder content (%)	≤15	14.2	9.8
Angularity test (s)	≥30	35.9	38.3
Apparent density (kg/m^3)	/	2.704	2.731
Water absorption (%)	/	2.1	1.5
Less than 0.075 mm particles (%)	≤15	8.6	8.2
Organic matter content	/	Qualified	Qualified
Trioxide content (%)	≤0.25	0.079	0.061

2.2. Mixing Proportion Trial of the LMR-CSPB

To reduce the test deviation, the proportion of each raw material was determined based on its screening test. Then the standard sieve (pore size: 19 mm, 9.5 mm, 4.75 mm, 2.36 mm) was used to weigh each raw material in proportion to form a mixed aggregate of LMR-CSPB.

The aggregate combination of LMR-CSPB material is listed in Table 6. A unified grading was used in the mixing proportion trial when the aggregate was selected to avoid the difference in gradation from affecting the test results and to ensure the validity of the test data. The requirements of aggregate gradation for LMR-CSPB materials are shown in Table 7.

Table 6. Aggregate combination mode in LMR-CSPB.

Aggregate Combination Mode	Coarse Aggregate	Fine Aggregate
A	Low-grade metamorphic rock	Low-grade metamorphic rock
B	Limestone	Limestone
C	Low-grade metamorphic rock	Limestone

Note: The gradations of limestone coarse aggregate and fine aggregate were adjusted to be the same as those of LMR rock aggregates to avoid the influence of gradations.

Table 7. Uniform grading requirements for LMR-CSPB.

Key Sieve (mm)	19	9.5	4.75	2.36	0.075
Passing ratio (%)	80	50	30	20	0~6

The content of cement in CSPB varies from 3% to 6% in mass. Detailed mix proportions are shown in Table 8.

Table 8. Mix proportions of CSPB.

Test Plan	Cement Dosage							
	3%		4%		5%		6%	
	M Value	O Value	M Value	O Value	M Value	O Value	M Value	O Value
A	2.34	5.2	2.34	5.2	2.33	5.3	2.34	5.3
B	2.26	5.0	2.27	5.0	2.28	5.1	2.29	5.1
C	2.32	5.1	2.32	5.1	2.33	5.2	2.34	5.2

Note: In the above table, the "M value" refers to maximum dry density, and its unit is g/cm^3; the "O value" refers to optimal water content, and its unit is %.

2.3. Methods

2.3.1. Compressive Strength

Strength is one of the most important performance indicators for the pavement performance of CSPB materials. To verify the strength properties of Base metamorphic rocks as road pavement material, LCR-CSPB specimens with the dimension of φ150 mm × 150 mm were prepared and cured under standard and dry–wet cycle curing conditions, respectively. The strength was measured at 7d, 14d, and 28d, respectively, according to JTG E51 [23].

2.3.2. Accelerated Simulation Experiment

The two ends of the CSPB specimen were cut flat and then dried in an oven. After the epoxy resin was completely cured, the initial test length of the CSPB specimen was measured and placed in a constant temperature water bath at 80 °C for curing. After 24 h, the specimen was taken out, and its reference length was quickly measured. Then specimens were cured in an 80 °C, 1 mol/L NaOH solution. Finally, the expansion rate of the CSPB specimen was tested at 3d, 7d, 10d, 14d, and 28d, respectively.

2.3.3. Microscopic Observation

A field emission scanning electron microscope (FESEM, Zeiss Ultra Plus) was employed to observe the microstructure of hydration products and cracks in the interface transition zone (ITZ) of concretes.

3. Results and Discussion

3.1. Trial Calculation of Total Alkali Content in CSPB

There is a specialized calculation method for the alkali content in CSPB using the relevant standards in China and abroad. The calculation method of the total alkali content of concrete is the sum of the alkali content of each constituent material (cement, admixtures, mineral admixtures, etc.) in the concrete. Therefore, the alkali content of CSPB is calculated by referring to Formula (1), which is consistent with the formula of concrete. The results for the total alkali content of different structures are shown in Table 9.

$$m_a = (m_c + 10) \times (c_c + 0.1\%) + m_{ca} \times c_{ca} + m_{ma} \times c_{ma} \quad (1)$$

where m_a is the total alkali in concrete (kg/m^3); m_c is the amount of cement in concrete (kg/m^3); m_{ca} is the amount of admixture in concrete (kg/m^3); m_{ma} is the amount of mineral admixture in concrete (kg/m^3); C_c is the effective alkali content of cement, and it is calculated as 100% of the alkali content of the cement (%); C_{ca} is the effective alkali content of admixture, and it is calculated as 100% of the alkali content of the admixture (%); and C_{ma} is the effective alkali content of the mineral admixture (%).

Table 9. Total alkali content of various structures.

Type	C30 Concrete	Concrete Pavement	Rolling Poor Concrete Base	Cement-stabilized Pavement Base
Cement (kg/m^3)	360	400	170	80
Cement ratio (%)	16.2	23.5	7.7	3.5
Total alkali content (kg/m^3)	1.94	2.00	0.85	0.45

Note: The cement ratio refers to the ratio of cement mass to the total mass of cements and aggregates. The alkali content of the cement in cement-stabilized pavement base is calculated as 0.56%.

Using the calculation, the 20% alkali content of fly ash is considered its effective alkali content, and the effective alkali content of silica fume and granulated blast furnace slag powder can be calculated as 50% of their alkali content. However, the effective alkali content of other mineral admixtures should be determined through experiments. The value of 0.1% is the supplementary amount for the effective alkali content to compensate for the fluctuations in the alkali content of the cement.

From Table 9, the total alkali content of CSPB is lower than other groups of concrete structures. At 0.45 kg/m^3, this is much less than the level (not more than 3 kg/m^3) that induces AAR [24]. The main reason is that the cement content of CSPB is generally between 3–6% by mass, which is much less than that of other concrete structures. Therefore, its total alkali content is lower than other concrete structures, and it does not meet a necessary condition for the alkali–aggregate reaction of "sufficient soluble alkali in the concrete pore solution".

3.2. Strength of the LMR-CSPB

The strength of CSPB specimens under different curing environments and cement dosages is illustrated in Figure 2. It is clear that under different curing ages, the strength of CSPB specimens in standard maintenance is better than that in a dry–wet cycle curing environment. Under the same curing environment, strength increases with the extension of the curing age and with the increase in cement dosages. At the same time, the strength of all CSPB specimens is greater than the design value of 4.0 MPa under different curing environments, cement contents, and curing ages, which meets the design requirements in JTG/T F20.

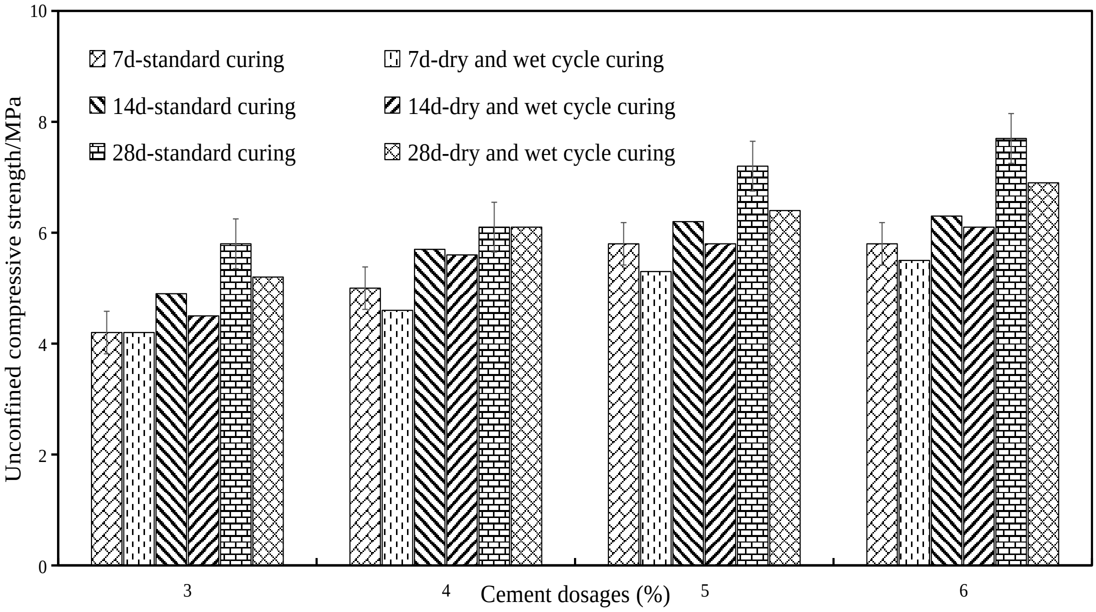

Figure 2. The strength of CSPB specimens under different curing environments and cement dosage.

To analyze the difference in strength performance of CSPB material prepared from LMR as aggregate and other commonly used rock aggregates, limestone was used as a control group for testing, and the 4% cement dosage was selected in the experiment. Figure 3 illustrates that the strength of CSPB specimens with LMR is similar to that of limestone CSPB specimens in standard maintenance and dry–wet cycle curing environments. This shows that LMR can replace general stone as aggregate to prepare CSPB material, and it meets the strength requirements. Therefore, it is feasible to use LMR as aggregate to prepare CSPB.

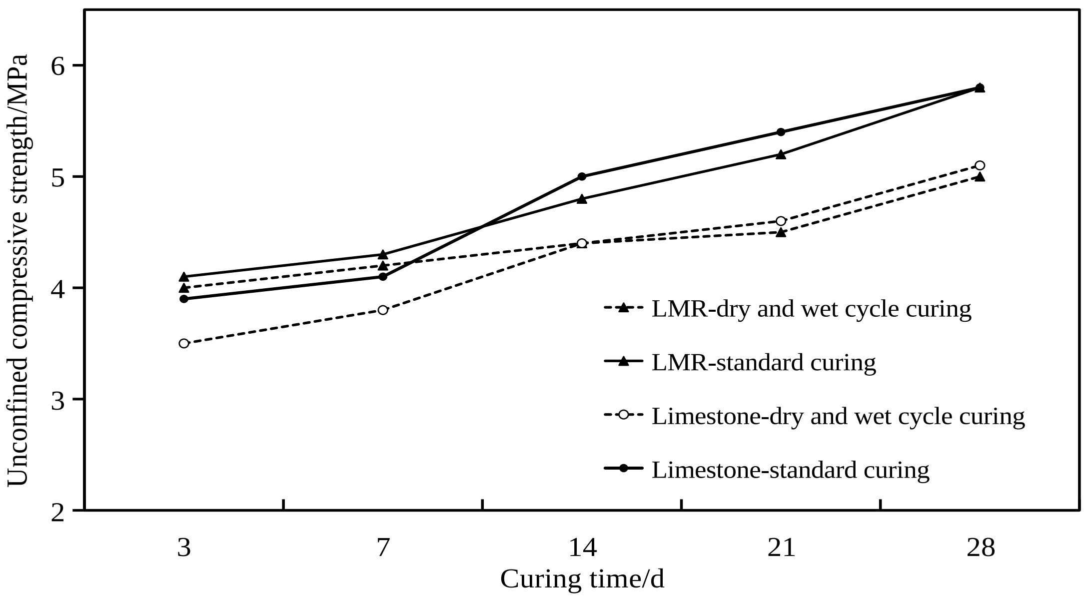

Figure 3. The strength of CSPB specimens with LMR and limestone aggregates.

3.3. Accelerated Simulation Experiment

Expansion rates of LMR-CSPB from the mortar bar method are shown in Figure 4. It is clear that the expansion of LMR-CSPB specimens increases with the curing time regardless of the cement dosage. However, the 14-d expansion rate of all specimens is less than 0.1%, which indicates that no AAR occurred in the LMR-CSPB specimens. The main reason is that the amount of cement used is very small, and its total alkali content is low. A sufficient alkaline solution environment for AAR is not provided in LMR-CSPB. Therefore, it will not cause the occurrence of AAR when the LMR is used in the CSPB within the cement dosage of 6%.

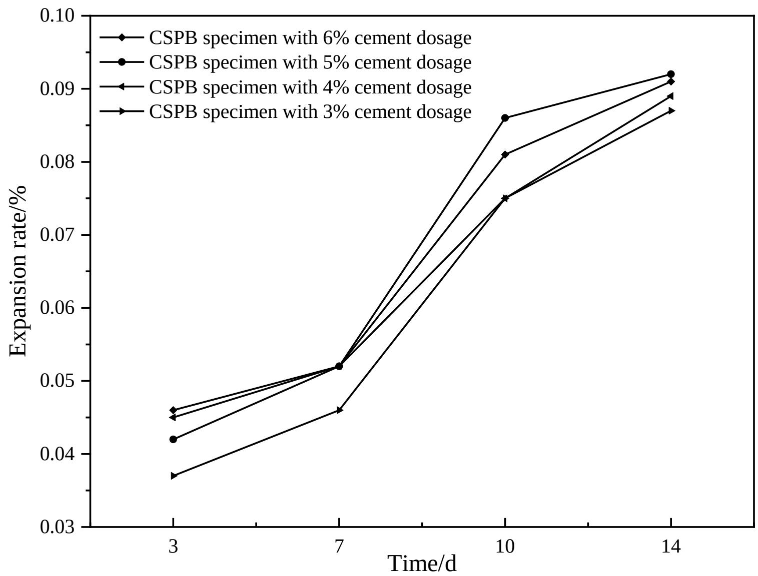

Figure 4. Accelerated simulation test results of the expansion rate of LMR-CSPB specimens.

3.4. Microscopic Observation

The AAR can be divided into alkali-silicic acid reaction (ASR) and alkali-carbonate reaction (ACR) according to the different types of alkali active minerals in the aggregate [25]. For shallow metamorphic rock aggregates, if alkali–aggregate reaction occurs, it is mostly ASR because of the high content of SiO_2. The principle of ASR is that the active SiO_2 in the aggregate reacts with the alkali in the pore solution, forming an alkali-silicic acid gel in the transition zone of the interface between the aggregate and the cement paste. The ASR product is mostly honeycomb-shaped gel with high water absorption. When the stress caused by swelling due to water absorption exceeds the strength of the concrete, it will cause the concrete to crack [26,27]. Therefore, whether there is an alkali aggregate reaction can be judged by observing the morphology around the aggregate and analyzing the product composition in the transition zone between the aggregate and the cement paste.

The morphologies of LMR-CSPB are shown in Figure 5. Figure 5a,b present the bonding state of the ITZ in the LRM-CSPB and L-CSPB specimens. It is obvious that the bonding between the aggregate and the cement paste is relatively close, and the structure is compact for both LMR-CSPB and L-CSPB. In L-CSPB specimens, an obvious crack is found at the edge of the aggregate. However, there is no crack in the interface of LRM-CSPB specimens. Magnified observation and analysis of the transition zone between the aggregate and the cement paste were carried out to clarify whether the crack is caused by AAR (see Figure 5c,d). The distribution of hydration products in the ITZ of LRM-CSPB and L-CSPB specimens is illustrated in Figure 5e,f. From Figure 5d,f, it can be seen that there is calcium hydroxide and ettringite hydrate in the crack, and there is no honeycomb alkali-silicate gel. At the same time, there are obvious rod-shaped ettringite crystals (AFt), hexagonal calcium hydroxide, and amorphous or agglomerated C-S-H gel products in the L-CSPB specimens. In addition, no AAR product can be observed.

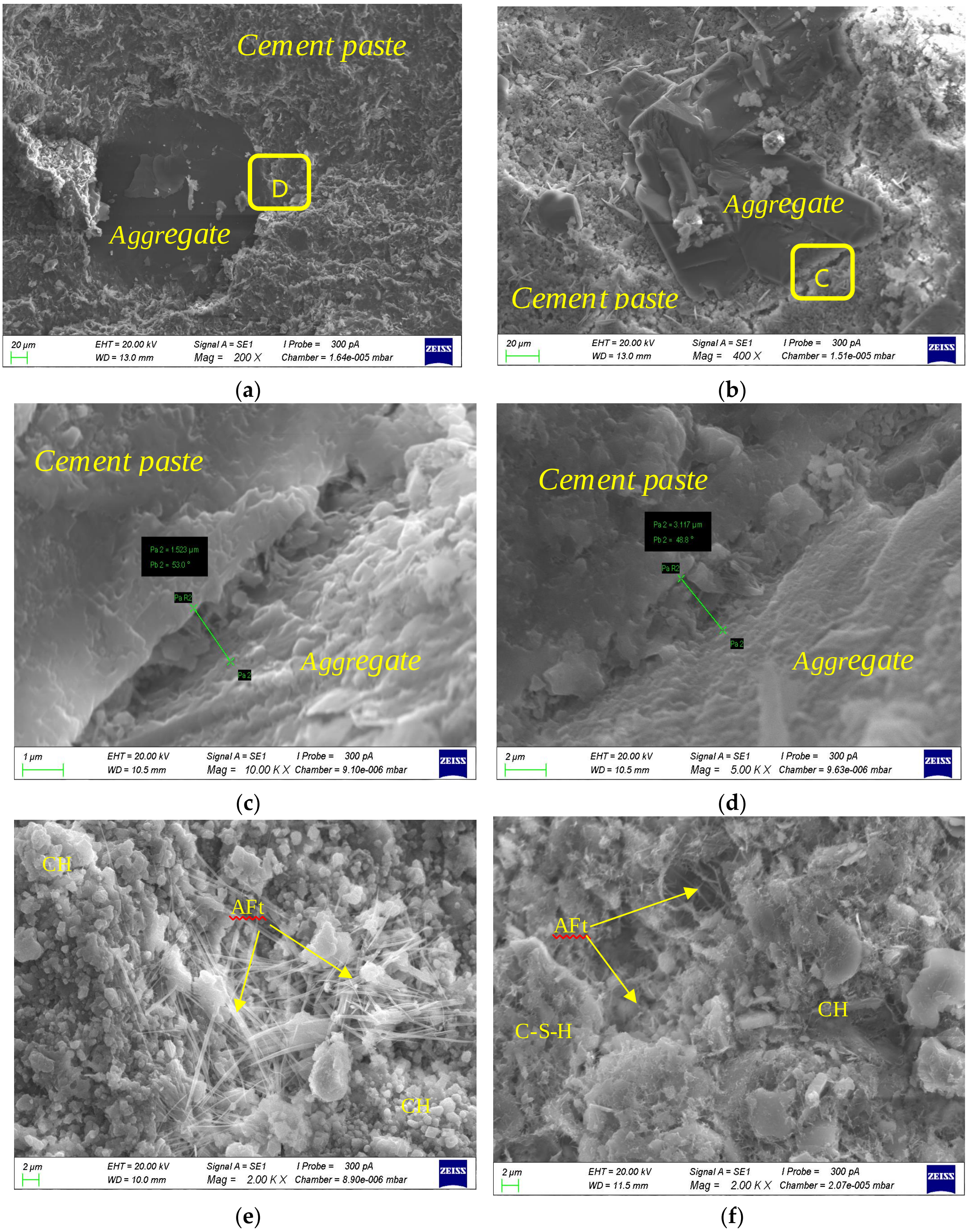

Figure 5. Sample microscopic analysis: (**a**) bonding of aggregate and cement in LMR-CSPB; (**b**) bonding of aggregate and cement in L-CSPB; (**c**) the ITZ of LMR-CSPB; (**d**) the ITZ of L-CSPB; (**e**) the hydration products in the LMR-CSPB; (**f**) the hydration products in the L-CSPB.

Similarly, the honeycomb-shaped alkali-silicate gel was not found in the ITZ of LMR-SCPB specimens, as shown in Figure 5e. There are obvious ettringite crystals, calcium hydroxide, and C-S-H gel in the LMR-CSPB specimens, and the adhesion is tight (Figure 5f). Comparison with the L-CSPB specimens shows that the LMR can be used as the raw material for the preparation of CSPB, and its strength meets the requirements of engineering design.

3.5. Economic and Environmental Analyses

Compared with the ordinary cement-stabilized pavement base, the technical and economic analysis of preparing one cubic meter of LMR-CSPB is shown in Table 10. As can be seen, the cost of one cubic meter of ordinary cement-stabilized pavement base and LMR-CSPB are about CNY 2705.18 and CNY 787.20, respectively. The LMR-CSPB can save 70.9% of the cost of an ordinary cement-stabilized pavement base.

Table 10. The technical and economic analysis of preparing LMR-CSPB.

Raw Materials	L-CSPB/m^3		LMR-CSPB/m^3		LMR-CSPB/m^3			L-CSPB/m^3		
	Dosage/t	Unit Price CNY(USD)/t	Dosage/t	Unit Price CNY(USD)/t	Dosage/t	Shipping Cost CNY(USD)/t	Unit Price CNY(USD)/t	Dosage/t	Shipping Cost CNY(USD)/t	Unit Price CNY(USD)/t
Manufactured sand	1	33(5.10)	1	40(6.18)	5.33	0	40(6.18)	5.33	103 (15.92)	136 (21.03)
Gravel	1	35(5.41)	1	40(6.18)	14.35	0	40(6.18)	14.35	103 (15.92)	138 (21.33)
Total cost CNY(USD)/m^3	-		-			787.2 (121.70)			2705.12 (418.21)	
Cost saving/%						70.9				

Note: CNY is a unit of RMB, which is converted to USD at 0.1546 rates. Economic benefit of the cement-stabilized pavement base with low-grade metamorphic rock is relative to ordinary cement-stabilized pavement.

In addition, the preparation of LMR-CSPB can involve the recycling of waste resources, such as shallow metamorphic rocks. It can also promote the scientific utilization of shallow metamorphic rock in the pavement base layer, which can improve the quality of construction and operation of the project and make the application of LMR-CSPB material on the pavement in areas enriched with shallow metamorphic rocks reach a new level. This promotes the sustainable development of engineering construction in areas enriched with shallow metamorphic rocks. Thus, it is summarized that LMR-CSPB has a great engineering significance and economic value, and its application prospects are very broad.

From the environmental viewpoint, the replacement of river sand with manufactured sand can eliminate severe impacts in river basin environments, such as decreased species diversity and biomass of aquatic organisms [28,29]. In addition, the replacement of locally-produced LMR aggregate for far-shipped river or manufactured limestone sand not only makes use of local resources but also reduces CO_2 emissions due to transportation.

4. Conclusions

This paper investigates the possibility of using LMR in CSPB, given that the alkali content of CSPB is low compared to traditional concrete due to the limited usage of concrete. Based on the findings, the main conclusions can be drawn as follows:

1. The total alkali content of CSPB is 0.45 kg/m^3, which is lower than the required value (normally higher than 3.0 kg/m^3), for triggering AAR.
2. CSPB has a higher compressive strength with a higher content of cement. In addition, the compressive strength of CSPB prepared with LMR is similar to that of limestone aggregate regardless of standard curing or wet–dry curing.
3. An accelerated simulation test demonstrated that there is no AAR in LMR-CSPB, given that the 14-d expansion rates are lower than 0.1% for all mixtures. This was further validated by microscopic analysis showing that no AAR product was found in any area of LMR-CSPB.
4. LMR-CSPB has a cost 70.9% lower than ordinary cement-stabilized pavement base, demonstrating the significant benefit of using LMR for the preparation of CSPB. Destruction of river basin environments can be avoided, and CO_2 emission caused by sand transportation can be reduced by using locally-produced LMR aggregate.

Therefore, it is concluded that LMR has a high potential to be used for preparing CSPB from technical, economic and environmental viewpoints.

Author Contributions: Conceptualization, Q.Y. and Z.J.; methodology, Y.L., H.Z., G.G. and Y.C.; software, H.Z.; formal analysis, Y.L., X.W. and L.Z.; investigation, Y.L., Y.C. and L.Z.; writing—original draft preparation, Y.L.; writing—review and editing, Z.J.; supervision, Q.Y.; project administration, Q.Y. All authors have read and agreed to the published version of the manuscript.

Funding: This project was financially supported by the Scientific Project Guizhou Province Transportation Office (2019-122-003), (2022-323-005), and the China Construction West Project (ZJXJ-2020-01). We also thank those factories for supplying raw materials for our research work.

Institutional Review Board Statement: Not applicable.

Informed Consent Statement: Not applicable.

Data Availability Statement: Not applicable.

Conflicts of Interest: The authors declare no conflict of interest.

References

1. Šťastná, A.; Šachlová, Š.; Pertold, Z.; Přikryl, R. Factors affecting alkali-reactivity of quartz-rich metamorphic rocks: Qualitative vs. quantitative microscopy. *Eng. Geol.* **2015**, *187*, 1–9.
2. Fournier, B.; Bérubé, M.A. Alkali–aggregate reaction in concrete: A review of basic concepts and engineering implications. *Can. J. Civ. Eng.* **2000**, *27*, 167–191. [CrossRef]
3. Bulteel, D.; Rafaï, N.; Degrugilliers, P.; Garcia-Diaz, E. Petrography study on altered flint aggregate by alkali–silica reaction. *Mater. Charact.* **2004**, *53*, 141–154. [CrossRef]
4. Broekmans, M.A.T.M. Deleterious reactions of aggregate with alkalis in concrete. *Rev. Mineral. Geochem.* **2012**, *74*, 279–364. [CrossRef]
5. Garcia-Diaz, E.; Riche, J.; Bulteel, D.; Vernet, C. Mechanism of damage for the alkali–silica reaction. *Cem. Concr. Res.* **2006**, *36*, 395–400. [CrossRef]
6. Stanton, T.E. Expansion of concrete through reaction between cement and aggregate. In Proceedings of the ASCE, Los Angeles, CA, USA, December 1940; Volume 66, pp. 1781–1811.
7. Tang, M.S. General situation of alkali-aggregate reaction in various countries in the world. *Cem. Eng.* **1999**, *4*, 1–6. (In Chinese)
8. Xu, H.; Chen, M. Alkali-Aggregate Reaction in Chinese Engineering Practices. *J. Yangtze River Sci. Res. Inst.* **1989**, *10*, 28–35.
9. Lin, L.; You, Y. The investigation and research of Alkali-Aggregaion reaction for Tianjin's concrete engineering. *J. Tianjin Urban Constr. Inst.* **2001**, *31*, 1015–1022. (In Chinese)
10. Qin, Y.; Xu, H.; Zhang, D. The research of restrain concrete alkali-aggregate reaction in Xinjiang area's buildings. *Sichuan Build. Sci.* **2009**, *22*, 941–948. (In Chinese)
11. Li, J.Y. Alkali aggregate reaction in dam concrete in China. *Hydroelectr. Power* **2005**, *31*, 34–37. (In Chinese)
12. Li, G.W.; Zhou, Q.W. Alkali-aggregate reaction of dam concrete of Jinping I Hydropower Station. In Proceedings of the Hydraulic Dam Concrete Materials and Temperature Control Academic Exchange Meeting, Chengdu, China, 6–9 July 2009. (In Chinese).
13. Deng, M.; Lan, X.; Xu, Z. Petrographic characteristics and distributions of reactive aggregates in China. In Proceedings of the 12th International Conference on Alkali-Aggregate Reaction in Concrete, Nanjing, China, 15–19 October 2004; Volume 1.
14. *ASTM C1260*; American Society for Testing and Materials. Philadelphia, American Society for Testing and Materials: West Conshohocken, PA, USA, 2011.
15. Bragg, D. Alkali-aggregate reactivity in Newfoundland, Canada. *Can. J. Civil. Eng.* **2000**, *27*, 192–203. [CrossRef]
16. Jiang, Z.W.; Li, X. Alkali reactivity of metamorphic rock aggregate and its prevention measures in the southeast area of Guizhou Province. *J. Build. Mater.* **2010**, *13*, 22–26. (In Chinese)
17. Wei, B. The engineering application and restraining technology for the alkali aggregate reaction of concretes with metamorphic rock aggregate. *J. China Foreign Highw.* **2014**, *51*, 761–769. (In Chinese)
18. Lu, D.; Fournier, B.; Grattan-Bellew, P. Evaluation of accelerated test methods for determining alkali-silica reactivity of concrete aggregates. *Cem. Concr. Comp.* **2006**, *28*, 546–554. [CrossRef]
19. Tayfur, S.; Yüksel, C.; Alver, N.; Akar, O.; Andiç-Çakır, Ö. Evaluation of alkali–silica reaction damage in concrete by using acoustic emission signal features and damage rating index: Damage monitoring on concrete prisms. *Mater. Struct.* **2021**, *54*, 1–17. [CrossRef]
20. Lee, W.E.; Gadow, R.; Mitic, V. Alkali-Aggregate Reactions in Concrete. In *Proceedings of the III Advanced Ceramics and Applications Conferenc*; Atlantis Press: Paris, France, 2016; pp. 221–240.
21. *TB/T 3275*; Concrete for Railway Construction. Industry Standards of People's Republic of China: Beijing, China, 2018.
22. *JTG/T F20*; Technical Guidelines for Construction of Highway Roadbases. Industry Standards of People's Republic of China: Beijing, China, 2015.
23. *JTG E51*; Test Methods of Materials Stabilized with Inorganic Binders for Highway Engineering. Industry Standards of People's Republic of China: Beijing, China, 2009.
24. *GB/T 50733*; Technical Specification for the Prevention of Alkali-Aggregate Reaction in Concrete. National Standards of People's Republic of China: Beijing, China, 2011.
25. García-Lodeiro, I.; Palomo, A.; Fernández-Jiménez, A. Alkali–aggregate reaction in activated fly ash systems. *Cem. Concr. Res.* **2007**, *37*, 175–183. [CrossRef]
26. Zhang, X.Y.; Gallucci, E.; Scrivener, K. Prognosis of Alkali Aggregate Reaction with SEM. *Adv. Mater. Res.* **2011**, *194*, 1012–1016. [CrossRef]

27. Grimal, E.; Sellier, A.; Pape, Y.L. Creep, Shrinkage, and Anisotropic Damage in Alkali-Aggregate Reaction Swelling Mechanism-Part I: A Constitutive Model. *Aci. Mater. J.* **2008**, *105*, 227–235.
28. Xu, F.; Jia, Y.; Wang, Y.; Zhang, F.; Li, L.; Li, Y.; Ren, L.; Wang, D.; Zhang, T. Does sand mining affect the remobilization of copper and zinc in sediments?—A case study of the Jialing River (China). *Environ. Res.* **2021**, *200*, 111416. [CrossRef] [PubMed]
29. Meng, X.; Jiang, X.; Li, Z.; Wang, J.; Cooper, K.M.; Xie, Z. Responses of macroinvertebrates and local environment to short-term commercial sand dredging practices in a flood-plain lake. *Sci. Total Environ.* **2018**, *631*, 1350–1359. [CrossRef] [PubMed]